NUCLEAR PHYSICS AND SUPERNOVAE*

K. Langanke

Institute for Physics and Astronomy, University of Aarhus
DK-8000 Aarhus C, Denmark

(Received November 20, 1999)

The manuscript reviews several nuclear physics aspects of relevance for supernova simulations. In particular, it stresses the role played by stellar weak interaction rates in the presupernova collapse and the recent progress achieved to calculate these rates based on large-scale shell model calculations. It further discusses the 'hot neutrino bubble' above a newly formed neutron star in a type II supernova as the possible site of the nuclear r-process, pointing to several still open questions. Finally the possible role of neutrinos in this r-process scenario is investigated.

PACS numbers: 26.50.+x

1. The general picture

The general ideas of the synthesis of elements in the universe has been derived now more than 40 years ago by Burbidge, Burbidge, Fowler and Hoyle [1] and, independently, by Cameron [2]. Due to this picture, the light elements (mainly hydrogen and helium) have been made during the Big Bang, while the breeding places for most of the other elements are stars. The stars generate the energy, which allows them to stabilize and shine for millions of years and longer, by transmuting nuclear species, thus forming new elements. These processes occur inside the star, but are eventually released if the star for example is massive enough and finally explodes in a type II supernova. The freshly bred nuclear material is mixed into the interstellar medium (ISM) and can thus become part of the initial abundance composition for a new star to be formed. Thus the galactical chemical evolution represents a 'cosmic cycle', and the modellation of the observed solar abundances (*e.g.* [3]) requires the simulations of the formation of a galaxy and of the stellar mass distribution, birth rates, evolution and lifetimes. Importantly one has to calculate the abundances produced by a star of a given

* Invited talk presented at the XXVI Mazurian Lakes School of Physics, Krzyże, Poland, September 1–11, 1999.

mass and the amount and composition of matter ejected into the ISM by the star's final type II supernova explosion. Finally contributions of type Ia supernovae have to be added which involve the formation and evolution of binary systems composed of a giant star with a hydrogen envelope and an accreting white dwarf.

During their lifetime stars go through various burning stages igniting nuclear fuel with increasingly higher charge numbers at increasingly higher densities and temperatures in the core (hydrogen, helium, carbon, neon, oxygen, silicon), while fuel with lower charge numbers are then burnt in shells in regions outside the core. Stars with masses $M < 10M_0$ (with the solar mass M_0) reach only conditions in the center which are sufficient for core helium burning; these stars produce mainly carbon, nitrogen, and half of the nuclei heavier than iron. More massive stars basically make the elements between oxygen and zinc, and, likely during their type II supernova explosion, also the other half of the elements heavier than iron. Finally, type Ia supernovae produce roughly half of the fraction of nuclei in the iron mass region, but also some portion of intermediate mass nuclei.

Despite its complexity, rather consistent studies of the galactical chemical evolution have been performed by Woosley and collaborators [4] and by Nomoto, Thielemann and collaborators [5]. Although the simulations involve still a few model assumptions (from the nuclear input, the rate of the important $^{12}C(\alpha,\gamma)^{16}O$ reaction is still too uncertain [6]), excellent agreement is obtained with solar abundances [7] for 76 isotopes from hydrogen to zinc, when the calculation is sampled at a time $4.55 \cdot 10^9$ years ago at a distance of 8.5 kpc from the galaxy center (corresponding to birth time and

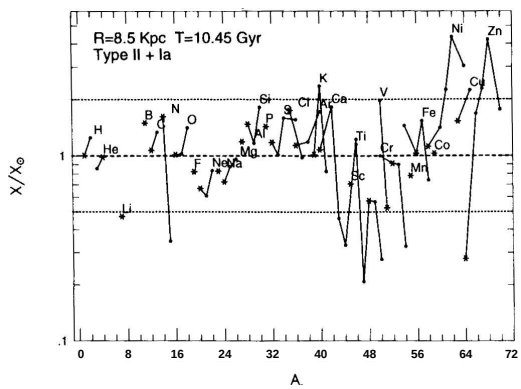

Fig. 1. Ratio of the calculated and observed solar abundances for stable isotopes from hydrogen to zinc. The dotted lines mark deviations by a factor of 2 between calculation and observation (from [4]).

position of our sun in the Milky Way). As can be seen in Fig. 1, most of the abundances agree within a factor of 2.

It should be mentioned that specific nuclei appear to be almost entirely (*e.g.* ^{11}B, ^{19}F) or in a large fraction (*e.g.* ^{10}B, ^{15}N) made by neutrino nucleosynthesis [8]. These nuclei are the product of reaction sequences induced by neutral current (ν, ν') reactions on very abundant nuclei like ^{12}C, ^{16}O and ^{20}Ne, when the flux of neutrinos generated by cooling of the neutron star passes through the overlying shells of heavy elements. Further, reactions between nuclei in the interstellar medium and high-energy cosmic rays contribute to the production of light elements (in particular Be and B isotopes).

2. Nuclear physics input in supernovae

Astrophysical environments can reach very high densities and temperatures. Under these conditions (temperatures T larger than a few 10^9 K), reactions mediated by the strong and electromagnetic force are in chemical equilibrium and the matter composition is given by nuclear statistical equilibrium, *i.e.* it is determined mainly due to the nuclear binding energies subject to the constraint that the total number of protons in the composition balances the number of electrons present in the environment. The parameter defining this constrain is the electron-to-baryon ratio Y_e. Importantly, in these astrophysical environments the relevant density and time scales are often such that the neutrinos are radiated away, so that reactions mediated by the weak interaction are not in equilibrium. Thus, weak interaction rates play a decisive role in these environments changing Y_e and hence the composition of the matter. Among these astrophysical environments are the two major distributors to the element production in the universe: supernovae of type Ia and type II (*e.g.* [9]).

2.1. Stellar weak interaction rates and type II supernovae

At the end of hydrostatic burning, a massive star consists of concentric shells that are the remnants of its previous burning phases (hydrogen, helium, carbon, neon, oxygen, silicon). Iron is the final stage of nuclear fusion in hydrostatic burning, as the synthesis of any heavier element from lighter elements does not release energy; rather, energy must be used up. If the iron core, formed in the center of the massive star, exceeds the Chandrasekhar mass limit of about 1.44 solar masses, electron degeneracy pressure cannot longer stabilize the core and it collapses starting what is called a type II supernova. In its aftermath the star explodes and parts of the iron core and the outer shells are ejected into the Interstellar Medium. Although this

general picture has been confirmed by the various observations from supernova SN1987a, simulations of the core collapse and the explosion are still far from being completely understood and robustly modelled. To improve the input which goes into the simulation of type II supernovae and to improve the models and their numerical simulations is a very active research field at various institutions worldwide.

As pointed out by Bethe *et al.* [10, 11] the collapse is very sensitive to the entropy and to the number of leptons per baryon, Y_e. In turn these two quantities are mainly determined by weak interaction processes, electron capture and β decay. First, in the early stage of the collapse Y_e is reduced as it is energetically favorable to capture electrons, which at the densities involved have Fermi energies of a few MeV, by (Fe-peak) nuclei. This reduces the electron pressure, thus accelerating the collapse, and shifts the distribution of nuclei present in the core to more neutron-rich material. Second, many of the nuclei present can also β decay. While this process is quite unimportant compared to electron capture for initial Y_e values around 0.5, it becomes increasingly competitive for neutron-rich nuclei due to an increase in phase space related to larger Q_β values.

Under the stellar conditions discussed above, the weak interaction rates are dominated by Gamow–Teller and, if applicable, by Fermi transitions. Bethe *et al.* [10] recognized the importance of the collective Gamow–Teller resonance for stellar electron capture. Shortly after, Fowler and Fuller outlined the theory for stellar weak-interaction rates. But as it then was impossible to solve the many-nucleon problem involved, these authors had to intuitively and empirically estimate the stellar electron capture and beta-decay rates (usually abbreviated as FFN, [12–15]. These FFN rates have been used by the astrophysics community until now.

It has been clear that the interacting shell model is the method of choice to solve the many-nucleon problem necessary to calculate the stellar weak-interaction rates. But only a couple of years ago, such a calculation appeared to be nearly impossible due to the extremely large model space dimensions to be considered (a few 10 millions or more). Impressive progress in both hardware technology and shell model diagonalization programming, however, allow now to treat these large shell model dimensions. Furthermore, relevant experimental data became available which can check the quality of the theoretical model. Within the last year it has been demonstrated that state-of-the-art shell model studies are indeed up to the job to reliably calculate the stellar weak-interaction rates as they reproduce all relevant ingredients very satisfying [16] (see Fig. 2). Having established the predictive power of the model, it has been used to calculate the weak-interaction rates (electron capture, β_- decay, but also positron capture and β_+ decay) for a wide range of astrophysical environment (temperatures up to $3 \cdot 10^{10}$ K and

densities up to 10^{10} g/cm^3) and for nuclei in the mass range $A = 45$–65. An electronic file of these shell model rates has been produced, using the same format in which the FFN rates are stored.

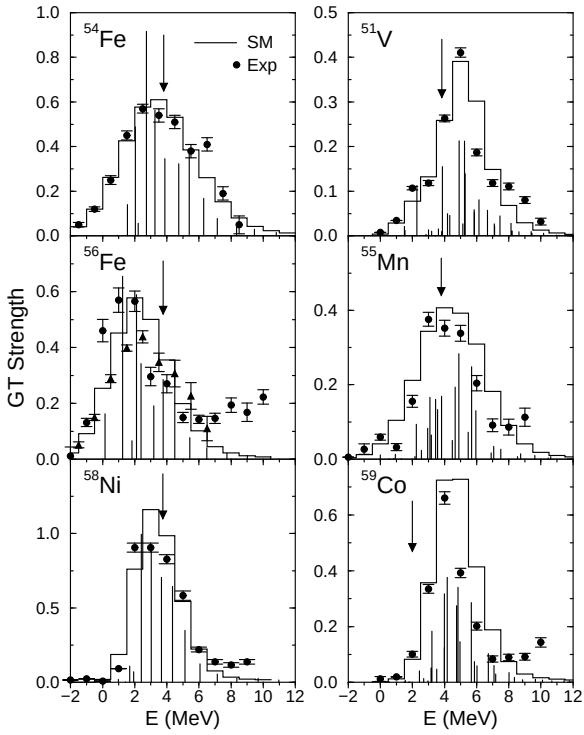

Fig. 2. Comparison of the shell model GT strength distribution (histogram) with data [18–22] for selected even–even (right) and odd-A nuclei (left). For the comparison the calculated discrete spectrum has been folded with the experimental resolution. The positions of the GT centroid assumed in the FFN parametrization are shown by arrows.

It is important to stress two important aspects of the shell model rates (see Fig. 3):

- The electron capture rates are significantly smaller than estimated by FFN (on average by more than an order of magnitude) along a stellar trajectory.
- The β decay rate exceeds the electron capture for values of $Y_e = 0.42$–0.46. This is also true for the FFN rates, but has not been explored yet, as older, statistical-model based β-decay rates have been used in collapse simulations.

The second finding allows for the exciting possibility to cool the core by emission of neutrinos without lowering Y_e. Taking both findings together, one expects that the Y_e value during the collapse is larger than currently assumed with interesting consequences for the actual collapse and supernova mechanism. This exciting possibility must be explored and it is hoped for that one might, for the first time, succeed to reliably calculate the entropy along the collapse trajectory.

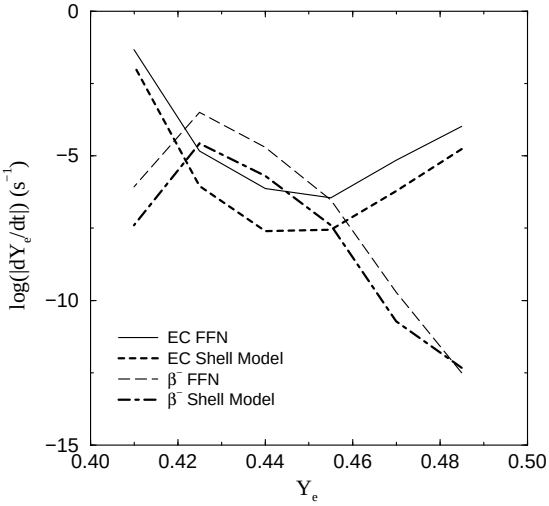

Fig. 3. Change in the total electron capture and β decay rates, $\dot{Y}_e^{ec}$ and $\dot{Y}_e^{\beta}$, respectively. The shell model results are compared with the FFN results [12–15] along the same stellar trajectory as in Fig. 14 of Ref. [26].

Electron capture, β decay and photodisintegration cost the core energy and reduce its electron density. As a consequence, the collapse is accelerated. An important change in the physics of the collapse occurs, if the density reaches $\rho_{\rm trap} \approx 4 \cdot 10^{11}$ g/cm^3. Then neutrinos are essentially trapped in the core, as their diffusion time (due to coherent elastic scattering on nuclei) becomes larger than the collapse time. After neutrino trapping, the collapse proceeds homologously [17], until nuclear densities ($\rho_N \approx 10^{14}$ g/cm^3) are reached. As nuclear matter has a finite compressibility, the homologous core decelerates and bounces in response to the increased nuclear matter pressure; this eventually drives an outgoing shock wave into the outer core; *i.e.* the envelope of the iron core outside the homologous core, which in the meantime has continued to fall inwards at supersonic speed. The core bounce with the formation of a shock wave is believed to be the mechanism that triggers a supernova explosion, but several ingredients of this physically

appealing picture and the actual mechanism of a supernova explosion are still uncertain and controversial. If the shock wave is strong enough not only to stop the collapse, but also to explode the outer burning shells of the star, one speaks about the 'prompt mechanism'. However, it appears as if the energy available to the shock is not sufficient, and the shock will store its energy in the outer core, for example, by excitation of nuclei.

After the supernova has exploded, a compact remnant is left behind. The remnant is very lepton-rich (electrons and neutrinos), the latter being trapped as their mean free paths in the dense matter is significantly shorter than the radius of the neutron star. It takes a fraction of a second [23] for the trapped neutrinos to diffuse out, giving most of their energy to the neutron star during that process and heating it up. The cooling of the protoneutron star then proceeds by pair production of neutrinos of all three generations which diffuse out. After several tens of seconds the star becomes transparent to neutrinos and the neutrino luminosity drops significantly [24]. In the 'delayed mechanism', the shock wave can be revived by these outward diffusing neutrinos, which carry most of the energy set free in the gravitational collapse of the core [25].

It is generally accepted that there is a temperature hierarchy between the various neutrino types introduced by the charged current reactions with the surrounding neutron-rich matter. Thus, μ and τ neutrinos and their antiparticles (usually combiningly referred to as ν_x neutrinos) have the distribution with the highest temperature ($T = 8$ MeV if one accepts a Fermi-Dirac distribution with zero chemical potential [8]). As the ν_e and $\bar{\nu}_e$ neutrinos interact with the neutron-rich matter via $\nu_e + n \rightarrow p + e^-$ and $\bar{\nu}_e + p \rightarrow n + e^+$, the $\bar{\nu}_e$ neutrinos have a higher temperature ($T \approx 5.6$ MeV) than the ν_e neutrinos ($T = 4$ MeV). It is useful for the following discussions to note that these temperatures correspond to average neutrino energies of $\bar{E}_\nu = 25$ MeV for ν_x neutrinos, while $\bar{E}_\nu = 16$ MeV and 11 MeV for $\bar{\nu}_e$ and ν_e neutrinos.

In the delayed supernova mechanism, neutrinos deposit energy in the layers between the nascent neutron star and the stalled prompt shock. This lasts for a few 100 ms, and requires about 1% of the neutrino energy to be converted into nuclear kinetic energy. The energy deposition increases the pressure behind the shock and the respective layers begin to expand, leaving between shock front and neutron star surface a region of low density, but rather high temperature. This region is called the 'hot neutrino bubble' and, as we will discuss below, might be the site of the nuclear r-process. The persistent energy input by neutrinos keeps the pressure high in this region and drives the shock outwards again, eventually leading to a supernova explosion.

It has been found that the delayed supernova mechanism is quite sensitive to physics details deciding about success or failure in the simulation

of the explosion. Very recently, two quite distinct improvements have been proposed (convective energy transport [27,28] and in-medium modifications of the neutrino opacities [29,30]) which should make the explosion mechanism more robust, as they increase the efficiency of the energy transport to the stalled shock.

2.2. Stellar weak interaction rates and type Ia supernovae

A type Ia supernova is usually associated with a thermonuclear explosion on a white dwarf, which accretes mass from a companion star in a binary system. This mass flow increases the density and temperature in the core so that finally carbon is ignited in the center of the star. Note that in a highly degenerate object like a white dwarf the energy release of the nuclear burning is used to increase the temperature (rather than for expansion as during hydrostatic stellar burning), which in turn drastically increases the nuclear reaction rates. Finally a thermonuclear runaway is triggered and a burning front then moves outwards through the star at subsonic speed, finally leading to a detonation which explodes the star. It appears well established that electron capture will occur in the burning front driving the matter to larger neutron excess and thus strongly influences the composition of the ejected matter and the dynamics of the explosion.

Although the general picture of a type Ia supernova might be developed, special issues are currently still under debate [31]. This includes the masses of the stars in the binary system, the mass accretion history and composition, the matter transport during the explosion, and the speed of the burning front. These quantities have to be modelled and the resulting output (elemental abundances and their velocity distributions) is compared to observation allowing to check the models. However, the results are also strongly affected by the weak-interaction rates and the shell model rates promise to remove this additional uncertainty from the models. Preliminary studies, performed with Thielemann's group, look very promising as the new rates apparently remove the overproduction of very neutron-rich isotopes, encountered in previous calculations with the FFN rates [32].

2.3. Future work on stellar weak interaction rates

Although the availability of the shell model rates for the mass range $A = 45$–65 is considered decisive progress in the community of supernova modellers, it is not sufficient. Electron capture already occurs during oxygen and silicon burning, implying the need to extend the rates to lighter nuclei ($A < 45$). Further a core collapse supernova might reduce the Y_e value before neutrino trapping to such low values ($Y_e \leq 0.44$) that nuclei with $A > 65$

become abundant in the matter composition, and hence weak-interaction rates for these heavier nuclei are also needed.

To extend the shell model studies to lighter or heavier nuclei than considered by us so far, brings in new physics and new challenges. In both cases calculations within model spaces spanned by one major shell, which is adequate for the nuclei with $A = 45$–65, is not sufficient. For the lighter nuclei one has to include the orbitals from the lower *sd* shell, while for heavier nuclei the $g_{9/2}$ orbital has to be considered. This enlargement to two major shells can excite unphysical center-of-mass degrees of freedom. However, the machinery to avoid such spurious excitations is at hand. Secondly, novel effective interactions among the valence particles have to be developed and tested.

The calculation of the electron capture rates for heavier nuclei with neutron numbers larger than $N > 40$ involves also an interesting physics aspect. Note that the Gamow–Teller operator $\vec{\sigma}\tau$, which mediates the electron capture transitions under stellar conditions, only acts on the spin and isospin degrees of freedom, but not on the spatial wave function. Thus, the Gamow–Teller operator can only move nucleons between orbitals in the *same* major shell. This means that for nuclei with proton number $Z < 40$ and neutron number $N > 40$, Gamow–Teller transitions are identical zero ('Pauli blocked') in electron capture, as $N = 40$ corresponds to the closed shell configuration. It is argued that electron capture during a supernova collapse shifts from capture on nuclei to capture on free protons, if nuclei dominate the matter composition for which the Gamow–Teller transition is Pauli-blocked. As discussed by Bethe [11] this situation can be overcome by thermal excitation moving protons into orbitals of the next higher shell or by removing neutrons of the otherwise blocked shell [33]. But, the 'thermal unblocking' requires rather high temperatures ($T > 10^{10}$K). However, there is another unblocking mechanism, so far overlooked. The residual interaction, in particular the pairing force among nucleons, also scatters protons and neutrons into the unblocked shell, thus having the same effect as the thermal unblocking. Importantly, this effect happens already at lower temperatures and thus we expect that the Gamow–Teller transitions are actually never blocked in the stellar electron capture, in contrast to the current believe.

3. The r-process

About half of the elements heavier than mass number $A = 60$ are made in the astrophysical r-process, a sequence of neutron capture and beta decay processes. The r-process is associated with environment of relatively high temperatures ($T \approx 10^9$ K) and very high neutron densities ($> 10^{20}$ neutrons/cm^3) such that the intervals between neutron captures are gener-

ally much smaller than the β lifetimes, *i.e.* $\tau_n \ll \tau_\beta$ in the r-process. Thus, nuclei are quickly transmuted into neutron-richer isotopes, decreasing the neutron separation energy B_n. This series of successive neutron captures comes to a stop when the (n,γ) capture rate for an isotope equals the rate of the destructive (γ,n) photodisintegration rate. Then the r-process has to wait for the most neutron-rich nuclei to β-decay. Under the typical conditions expected for the r-process, the $(n,\gamma)/(\gamma,n)$ equilibrium is achieved at neutron separation energies, $B_n = 2-3$ MeV [37]. This condition mainly determines the r-process path, which is located about 15-20 units away from the valley of stability. The r-process path reaches the neutron shell closures at $N_n = 50, 82$, and 126 at such low Z-values that B_n is too small to allow the formation of still more neutron-rich isotopes; the isotopes then have to β-decay. To overcome the shell gap at the magic neutron numbers and produce heavier nuclei, the material has to undergo a series of alternating β-decays and neutron captures before it reaches a nucleus close enough to stability to have B_n large enough to allow for the continuation of the sequence of neutron capture reactions. Noting that the β-decay half-lives are relatively long at the magic neutron numbers, the r-process network waits long enough at these neutron numbers to build up abundance peaks related to the mass numbers $A \approx 80, 130$, and 195. Simulations of the r-process require a knowledge of nuclear properties far from the valley of stability. As the relevant nuclei are not experimentally accessible, theoretical predictions for the relevant quantities (*i.e.* neutron separation energies and half-lives) are needed.

3.1. r-process in the hot neutrino bubble

Within the last few years the neutrino-driven wind model has been widely discussed as the possible site of r-process nucleosynthesis [34, 35]. Here it is assumed that the r-process occurs in the layers heated by neutrino emission and evaporating from the hot protoneutron star after core collapse. In this model (*e.g.* [36]), a hot blob of matter with entropy per baryon S_b and electron-to-baryon ratio Y_e, initially consisting of neutrons, protons and α-particles in nuclear statistical equilibrium (NSE), expands adiabatically and cools. Nucleons and nuclei combine to heavier nuclei, with some neutrons and α-particles remaining. Depending on the value of S_b, the nuclei produced are in the iron group or, at higher entropies, can have mass numbers $A = 80$–100. These nuclei then become the seeds and, together with the remaining neutrons, undergo an r-process [37]. In this model a successful r-process depends mainly on four parameters: the entropy per baryon S_b, the dynamical timescale, the mass loss rate and the electron-to-baryon ratio Y_e. All parameters depend on the neutrino luminosity and are determined

mostly by ν_e and $\bar{\nu}_e$ absorption on free nucleons. During a supernova explosion these parameters vary and the r-process in the hot neutrino bubble becomes a dynamical and time-dependent scenario. Woosley *et al.* [34] have calculated the r-process abundance for this site, adopting the parameters as given by Wilson's successful supernova model. The final abundances obtained after integration over the duration of the r-process in the hot neutrino bubble (several seconds) are shown in Fig. 4, showing quite satisfying agreement between calculation and observation.

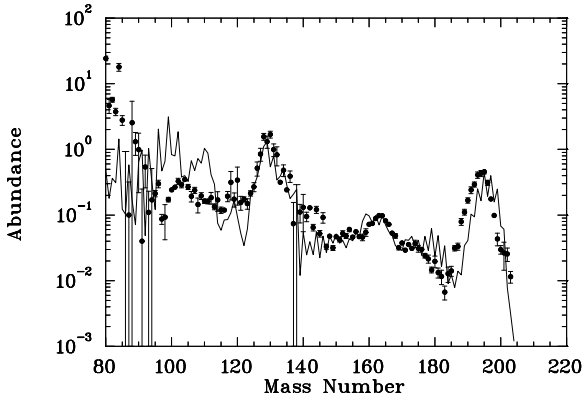

Fig. 4. r-process abundances in the hot neutrino bubble model compared to observation (from [34])

The open question currently is what kind of superpositions of entropies the supernova neutrino-driven wind environment really provides. In the supernova model used by Woosley et al [34] entropies up to $S_b = 300$ have been reached, but other models suggest that S_b is a factor of 3–5 smaller (*e.g.* [35]). To understand the importance of the entropy, one has to consider that the production of seed nuclei has to go through the bottleneck of the 3-body reaction $\alpha+\alpha+n \rightarrow {}^9\mathrm{Be}$ at the start. Due to the low Q-value of this reaction ($Q = 1.57$ MeV), a large entropy (or high photon number) drives this reaction in equilibrium to the left, ensuring a rather small amount of ${}^9\mathrm{Be}$. Since all ${}^9\mathrm{Be}$ is basically transformed into seed nuclei, a high entropy results in a small amount of seed nuclei and a large neutron-to-seed ratio n/s [38]. Systematic studies by Hoffmann and collaborators [39] and Freiburghaus *et al.* [36] have shown that a successful r-process requires either large entropies at the Y_e values currently obtained in supernova models, or smaller values for Y_e.

Furthermore the duration of the r-process, *i.e.* the minimal time required to transmute, at one site, seed nuclei into nuclei around $A \approx 200$,

is dominantly given by the sum of the half-lives of the r-process nuclei at the three magic neutron numbers. It appears as if the required minimal time is longer than the duration of the favorable r-process conditions in the neutrino-driven wind model. However, this problem might be overcome as recent calculations indicate the halflives of nuclei along the r-process path might be noticeably shorter than assumed so far.

3.2. Halflives of waiting point nuclei

The halflives of nuclei along the r-process path are determined by the weak low-energy tails of the Gamow–Teller strength distribution, mediated by the operator $\sigma\tau_-$, and provide quite a challenge to theoretical modelling as they are not constrained by sum rules. Previous estimates have been based on semi-empirical global models, quasiparticle random phase approximation, or very recently, the Hartree–Fock–Bogoliubov method [40–42]. But the method of choice to calculate Gamow–Teller transitions is the interacting nuclear shell model, and the decisive progress in programming and hardware make reliable shell model calculations of the halflives r-process nuclei now feasible.

In fact, the first series of shell model calculations, performed for the r-process waiting point nuclei with neutron number $N = 82$, has just been finished [43]. Experimental information is only available for ^{129}Ag and ^{130}Cd [44], and the shell model halflives agree well with the data, while the model predictions previously used in r-process simulations overestimate the data appreciably (see Fig. 5).

The shell model results might imply two important conclusions:

1) The time spent at the $N = 82$ waiting point is shorter than previously assumed (also supported by the recent HFB calculations [42]). This is highly welcome, as in the neutrino-driven wind model the longer theoretical halflive predictions made it very hard to transport matter from the light nuclei up to uranium during the dynamical timescale in which the neutron supply is high enough to allow a successful r-process.

2) Applying the approximate picture of a steady flow to the r-process network, observed elemental abundances should be proportional to the halflives. This is well fulfilled for the shell model halflives for the lighter waiting point nuclei with $N = 82$, but not including ^{130}Cd. As the systematics of neutron separation energies put this nucleus on the r-process path, our result suggests that the favorable r-process conditions do not last long enough to proceed to the $N = 126$ r-process peak under the same conditions at which the $N = 82$ peak is produced. This result is consistent with very recent meteoretic and astronomical

findings suggesting that the $N = 82$ and $N = 126$ r-process peaks are possibly made at two distinct sites.

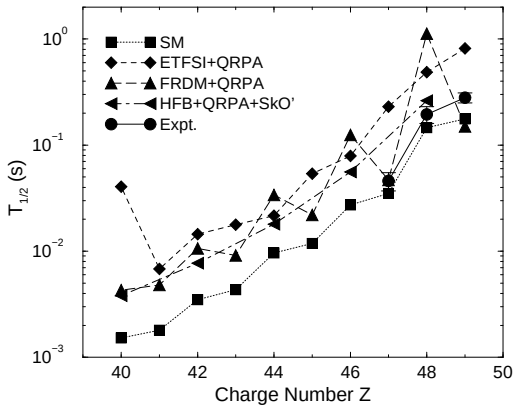

Fig. 5. Comparison of the shell model (SM) halflives for the $N = 82$ waiting point nuclei with data [44] and other model predictions [40–42]

Although these first shell model results are useful, consistent and firm conclusions can only be reached if shell model halflives are also available at least for the other two sets of waiting point nuclei related to the magic neutron numbers $N = 50$ and $N = 126$. These calculations are not straightforward, as the required model spaces reach the limits of what is currently possible on parallel computers.

3.3. Neutrino-induced reactions and the r-process

Neutrino-induced reactions can be important during and even after the r-process. In the conventional picture [37] the nuclei are basically in $(n, \gamma)/(\gamma, n)$ equilibrium during the r-process. The r-process path is mainly determined by neutron separation energies and the timescale is essentially set by the β-decays of the waiting-point nuclei at the magic neutron numbers $N = 50, 82$ and 126. However, in the presence of a strong neutrino flux, ν_e-induced charged-current reactions on the waiting-point nuclei might actually compete with β-decays and speed-up the passage through the bottle-necks at the magic neutron numbers [45]. It is found [45] that, for typical neutrino luminosities and spectra, ν_e-capture rates are of order 5 s^{-1} and thus can be faster than competing β-decays for the slowest waiting-point nuclei. Of course, quantitative conclusions can only be drawn from detailed numerical simulations of the r-process. A first step towards this goal has recently been made by Meyer *et al.* [46].

It is usually assumed that the r-process drops out of $(n,\gamma)/(\gamma,n)$ equilibrium in a sharp freeze-out. The very neutron-rich matter, assembled during the r-process, then decays back to the valley of stability by a sequence of β-decays. However, in the neutrino-driven wind scenario the r-process matter will still be exposed to rather strong neutrino fluxes, even after freeze-out. By both ν_e-induced charged-current and ν_x-induced neutral-current reactions, neutrinos can inelastically interact with r-process nuclei. In these processes the final nucleus will be in an excited state and most likely decay by the emission of one or several neutrons. Thus, this *post-processing* of r-process matter after freeze-out might effect the final r-process abundance. The neutrino post-processing effects depend on the neutrino-induced neutron knock-out cross sections, which Qian *et al.* [45] have calculated based on the continuum random phase approximation and the statistical model, and on the total neutrino fluence through the r-process ejecta following freeze-out.

The dominant features of the observed r-process abundance distribution are the peaks at $A \sim 130$ and 195, corresponding to the progenitor nuclei with $N = 82$ and 126 closed neutron shells. Haxton *et al.* find that 8 nuclei, lying in the window $A = 124$–126 and 183–187, are unusually sensitive to

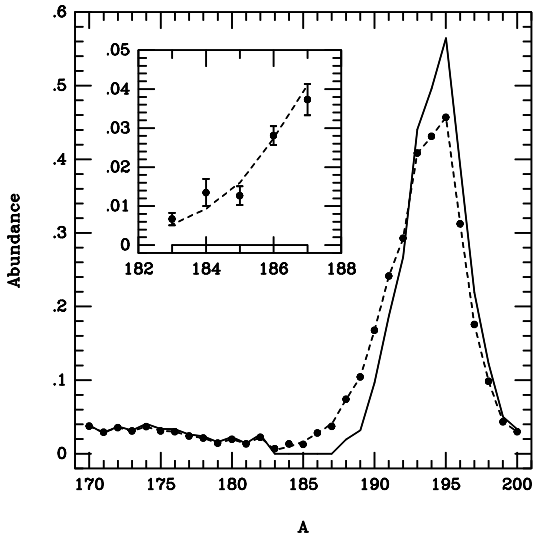

Fig. 6. Effect of postprocessing by neutrino-induced reactions on the r-process abundance. The unprocessed distribution (solid line) is compared with the distribution after postprocessing (dashed line). A constant fluence of $\mathcal{F} = 0.015$ has been assumed which provides a best fit to the observed abundances for $A = 183$–87 (see inset). The observed abundances are plotted as filled circles with error bars. (from [45])

neutrino post-processing [47]. These nuclei sit in the valleys immediately below the abundance peaks which can be readily filled by spallation of the abundant isotopes in the peaks. To avoid overproduction of the nuclei in these abundance windows one is able to place upper bounds on the fluence ($\mathcal{F} \leq 0.045$ at $A \sim 130$ and ≤ 0.030 at $A \sim 195$, respectively). Furthermore, it turns out that the observed abundance of the nuclei in the two abundance windows can be consistently reproduced by the same fluence parameter (for example see Fig. 6). This might be taken as evidence suggesting that the r-process does occur in an intense neutrino fluence, and thus that the interior region of a type II supernova is the site of the r-process.

We like to stress that the neutrino-induced knock-out liberates about 3–5 neutrons from nuclei in the abundance peaks around $A = 130$ and 195. Thus this process cannot be able to fill the well-developed abundance trough at $A \approx 115$ [48] where r-process simulations with conventional mass formulae strongly underestimate the observed abundances. This discrepancy might point to interesting nuclear structure effects in very neutron-rich nuclei, related to shell quenching far from stability [49].

It is a pleasure to thank G. Martinez-Pinedo whose collaboration has decisively contributed to the results presented in this manuscript. Many fruitful discussions with F.-K. Thielemann are gratefully acknowledged. The research has been partly supported by a grant of the Danish Research Council.

REFERENCES

[1] E.M. Burbidge, G.R. Burbidge, W.A. Fowler, F. Hoyle, *Rev. Mod. Phys.* **29**, 547 (1957).

[2] A.G.W. Cameron, Chalk River Report CRL-41 (1957).

[3] B.E.J. Pagel, G. Trautvaisiene, *Mon. Not. R. Astron. Soc.* **276**, 505 (1995); **288**, 108 (1997).

[4] F. Timmes, S.E. Woosley, T.A. Weaver, *Astrophys. J. Suppl.* **98**, 617 (1995).

[5] T. Tsujimoto, K. Nomoto, Y. Yoshii, M. Hashimoto, F.-K. Thielemann, *Math. Notes* **277**, 945 (1995).

[6] L. Buchmann, R.E. Azuma, C.A. Barnes, J. Humblet, K. Langanke, *Phys. Rev.* **C54**, 393 (1996) and references therein.

[7] E. Anders, N. Grevesse, *Geochim. Cosmochim. Acta* **53**, 197 (1989).

[8] S.E. Woosley, D. Hartmann, R.D. Hoffman, W.C. Haxton, *Astrophys. J.* **356**, 272 (1990).

[9] D. Arnett, *Supernovae and Nuclei*, Princeton University Press, 1996.

[10] H.A. Bethe, G.E. Brown, J. Applegate, J.M. Lattimer, *Nucl. Phys.* **A324**, 487 (1979).

[11] H.A. Bethe, *Rev. Mod. Phys.* **62**, 801 (1990).

[12] G.M. Fuller, W.A. Fowler, M.J. Newman, *Astrophys. J. Suppl.* **42**, 447 (1980).

[13] G.M. Fuller, W.A. Fowler, M.J. Newman, *Astrophys. J. Supplement* **48**, 279 (1982).

[14] G.M. Fuller, W.A. Fowler, M.J. Newman, *Astrophys. J.***252**, 715 (1982).

[15] G.M. Fuller, W.A. Fowler, M.J. Newman, *Astrophys. J.* **293**, 1 (1985).

[16] E. Caurier, K. Langanke, G. Martinez-Pinedo, F. Nowacki, *Nucl. Phys.* **A653**, 439 (1999).

[17] P.Goldreich, S.V. Weber, *Astrophys. J.* **238**, 991 (1980).

[18] A.L. Williams *et al.*, *Phys. Rev.* **C51**, 1144 (1995).

[19] W.P. Alford *et al.*, *Nucl. Phys.* **A514**, 49 (1990).

[20] M.C. Vetterli *et al.*, *Phys. Rev.* **C40**, 559 (1989).

[21] S. El-Kateb *et al.*, *Phys. Rev.* **C49**, 3129 (1994).

[22] T. Rönnquist *et al.*, *Nucl. Phys.* **A563**, 225 (1993).

[23] A. Burrows, *Ann. Rev. Nucl. Sci.* **40**, 181 (1990).

[24] A. Burrows, *Astrophys. J.* **334**, 891 (1988).

[25] J.R. Wilson, in *Numerical Astrophysics*, ed. by J.M. Centrella, J.M. LeBlanc and R.L. Bowers, Jones and Bartlett, Boston 1985, p.422.

[26] M.B. Aufderheide, I. Fushiki, S.E. Woosley, D.H. Hartmann, *Astrophys. J. Suppl.* **91**, 389 (1994).

[27] A. Burrows, B.A. Fryxell, *Science* **258**, 430 (1992).

[28] E. Müller, H.-T. Janka, *Astron. Astrophys.* **317**, 140 (1997).

[29] S. Reddy, M. Prakash, J.M. Lattimer, *Phys. Rev.* **D58**, 3009 (1998).

[30] A. Burrows, R.F. Sawyer, *Phys. Rev.* **C58**, 554 (1998).

[31] P. Ruiz-Lapuente, R. Canal, J. Isern, *Thermonuclear Supernovae*, Kluwer Academic Publishers, Dordrecht 1997.

[32] F. Brachwitz *et al.*, submitted to *Astrophys. J.*

[33] J. Cooperstein, J. Wambach, *Nucl. Phys.* **A420**, 591 (1984).

[34] S.E. Woosley, J.R. Wilson, G.J. Mathews, R.D. Hoffmann, B.S. Meyer, *Astrophys. J.* **433**, 229 (1994).

[35] J. Witti, H.-Th. Janka, K. Takahashi, *Astron. Astrophys.* **286**, 841; 857 (1994).

[36] F.-K. Thielemann, T. Rauscher, C. Freiburghaus, K. Nomoto, M. Hashimoto, B. Pfeiffer, K.-L. Kratz, to be published.

[37] J.J. Cowan, F.-K. Thielemann, J.W. Truran, *Phys. Rep.* **208**, 267 (1991).

[38] Y.-Z. Qian, S.E. Woosley, *Astrophys. J.* **471**, 331 (1996).

[39] R.D. Hofmann, S.E. Woosley, Y.-Z. Qian, *Astrophys. J.* **482**, 951 (1997).

[40] I.N. Borsov, S. Goriely, J.M. Pearson, *Nucl. Phys.* **A621**, 307c (1997).

[41] P. Möller, J.R. Nix, K.-L. Kratz, *At. Data Nucl. Data Tables* **66**, 131 (1997).

[42] J. Engel, M. Bender, J. Dobaczewski, W. Nazarewicz and R. Surman, *Phys. Rev.* **C60**, 014302 (1999).

[43] G. Martinez-Pinedo, K. Langanke, *Phys. Rev. Lett.*, **83**, 4502 (1999).

[44] K.-L. Kratz *et al.*, in *Proceedings of the International Conference on Fission and Properties of Neutron-Rich Nuclei*, ed. by J.H. Hamilton, World Scientific Press, 1998.

[45] Y.-Z. Qian, W.C. Haxton, K. Langanke, P. Vogel, *Phys. Rev.* **C55**, 1532 (1997).

[46] B.S. Meyer, G.C. McLaughlin, G.M. Fuller, *Phys. Rev.* **C58**, 3696 (1998).

[47] W.C. Haxton, K. Langanke, Y.-Z. Qian, P. Vogel, *Phys. Rev. Lett.* **78**, 2694 (1997).

[48] K.-L. Kratz, J.-P. Bitouzet, F.-K. Thielemann, P. Möller, B. Pfeiffer, *Astrophys. J.* **402**, 216 (1993).

[49] B. Chen, J. Dobaczewski, K.-L. Kratz, K. Langanke, B. Pfeiffer, F.-K. Thielemann, *Phys. Lett.* **B355**, 37 (1995).